Infrared Spectra of Silane in Solid Argon and Hydrogen

L. Li, J. T. Graham, and W. Weltner, Jr.*

Department of Chemistry, University of Florida, Gainesville, Florida 32611-7200

Received: August 2, 2001; In Final Form: October 2, 2001

After preliminary studies of CH_4 in solid argon and hydrogen, the infrared absorption spectra of matrix-isolated SiH_4 and SiD_4 in solid argon, hydrogen, and deuterium at 2−4 K were measured. The two infrared-active ν_4 (bending) and ν_3 (asymmetric stretching) regions were observed. The absence of bands due to absorption from the $J = 1$ excited rotational state in the ground vibrational level indicates that (1) the nuclear spin conversion is relatively rapid and (2) the silane molecules are not rotating or are highly hindered rotationally in these matrices at 2 and 4 K. The SiH_3 radical was observed in solid hydrogen; it was produced by photolysis of the silane/hydrogen matrix with radiation from a hydrogen discharge.

1. Introduction

The main objective of this research was to observe the rotation−vibration transitions of SiH_4 in solid hydrogen, with concern for nuclear spin conversion, just as Momose, Shida, et al., have recently done for CH_4. However, it was also expedient to make observations in argon, as representative of the rare gas matrixes, where there is an extensive background of work for CH_4,[1−21] but much less for SiH_4 and silyl radicals.[22−30] To test our procedure, which differed somewhat from previous work, we also observed spectra of CH_4.

Nuclear spin conversion in methane at low temperatures in solid methane[2,3,5,7] and the solid rare gases[1,4,6,9−11] has been thoroughly studied. In rare-gas matrices, the work most relevant to this research is by Frayer and Ewing (FE)[1], Hopkins et al.,[4] Baciocco et al.,[9] Jones et al. (JES),[10] and Jones and Eckberg[11] on CD_4. In solid hydrogen, there are the excellent studies of nuclear spin conversion of CH_4 by Momose et al. (MS),[13−17] and by high-resolution infrared spectroscopy by Momose et al.[18]

SiH_4 and SiH_3 have been observed spectroscopically in the gas phase,[31−36] and all of the SiH_x hydride molecules have been theoretically studied by Allen and Schaefer.[37] A thorough investigation of the infrared spectra of SiH_4 and its deuterated species in solid Ne, Ar, Kr, Xe, N_2, CO, and CH_4 was made in 1971 by Wilde et al. (WSHS)[22] with matrix-to-sample ratios of 50 to 5000. Later, IR spectra were also obtained in Ar by Abouaf-Marguin and Lloret.[24,29]

Here we repeat the measurements of WSHS at higher dilution and higher resolution in solid Ar and extend them to hydrogen matrices. A further objective was the formation of SiH_3 from SiH_4 by photolysis and condensation in hydrogen.

Nuclear Spin Conversion. This has been considered by FE[1], JES,[10] and MS[13−17] for CH_4. In the absence of a paramagnetic impurity, rapid deposition from room temperature to 4 K would lead to a relative population of $J = 1$ to $J = 0$ in the lowest vibrational level of about 2 to 1. In the absence of a catalyst (such as O_2), the transitions P(1), Q(1), R(1) are then relatively strong. ($J = 2$, 3 levels rapidly interconvert, and at 4 K transitions from them are not observed.)

Spin relaxation from the $J = 1$ state, either slowly, or rapidly via a catalyst, leads to a Boltzmann distribution, which at 4 K is a population ratio of $J = 1/J = 0$ of about 0.07 for CH_4 ($\tilde{B} = 5.2$ cm^{-1}). For SiH_4 this equilibrium population ratio would be about 0.37 (since $\tilde{B} = 2.9$ cm^{-1}). If rotating at 4 K after complete spin conversion, the transitions from the $J = 1$ level should still be readily observed. However, at 2 K the population ratio in $J = 1/J = 0$ becomes ∼0.05 for SiH_4, which, when spread over P(1) to R(1), makes these bands very small relative to R(0). If uncatalyzed, the observation of the variation of relative intensities with time is informative of the intrinsic nuclear spin conversion rate.

A further consideration is the possibility that in some or all sites in the matrix the "rotationless 0−0 transition" could be observed, as was assigned by Redington and Milligan[38] for H_2O in solid Ar, Kr, and Xe. It would be at a lower frequency from R(0) by Q(1) − P(1) and therefore should be distinct and observable. Miki and Momose[20] note that they did not observe this transition for CH_4 in p-H_2.

2. Experimental Section

All matrices were prepared by the usual direct deposition from the gas phase onto a cold surface and not by solidification from the liquid as used by FE and MS. The matrices were deposited on a polished aluminum surface at 2 or 4 K, and spectra were measured by reflection of the IR beam in a Bruker 113V vacuum FTIR spectrometer, generally at a resolution of 0.2 cm^{-1}. The aluminum was in contact with a copper surface cooled to 4 K with liquid helium. A temperature of about 2 K was obtained by pumping the liquid helium with a Leybold Sogevac vacuum pump. A set of mirrors in the spectrometer directed the IR beam through a CsI window into the cryostat, and the returning beam then was directed to the MCT detector cooled with liquid nitrogen.

para-H_2 was prepared by the method of Steinhoff et al.[39] and passed into a 5-liter storage bulb.

SiH_4 (Matheson, 99.998% research grade), SiD_4 (Sigma-Aldrich, 98 atom % D, electronic grade), H_2 (Matheson, 99.9995% research grade), and D_2 (Cambridge Isotope Laboratories, 99.6% research grade) gases were used. Gas mixtures ranging from 0.005 mol % (M/A = 20 000) were prepared in 5 L glass bulbs and sprayed on the cooled polished aluminum surface through a stainless steel tube for deposition times varying from 1/2 to 1 h. (The procedure is the same as JES except that they pulsed the premixed gas onto a cooled CsBr window.)

10.1021/jp013003m CCC: $20.00 © 2001 American Chemical Society
Published on Web 11/17/2001

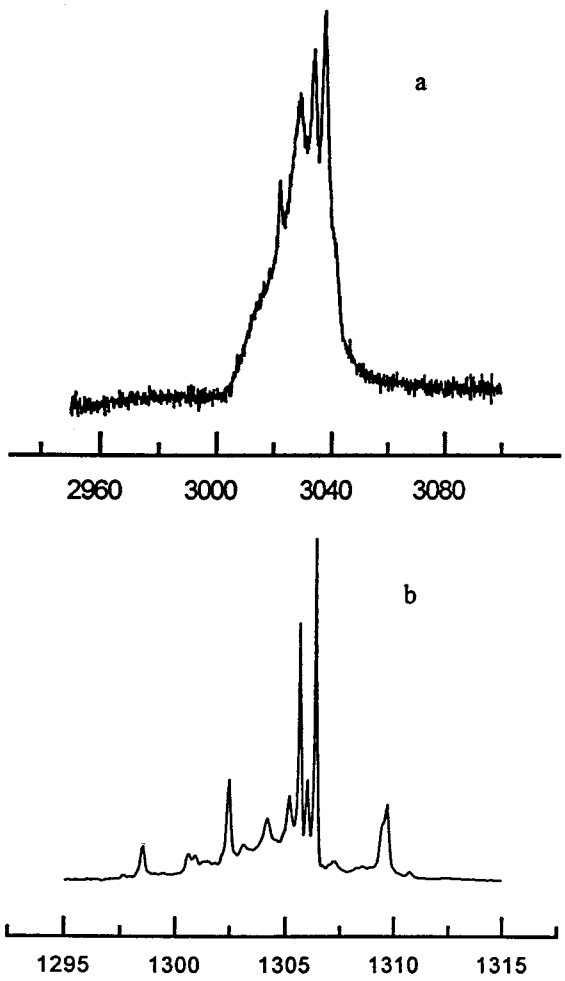

Figure 1. Absorption spectrum of 0.1 mol % (M/A = 1000) of CH_4 + 0.1% O_2 in solid argon at 4 K; (a) ν_3 region, (b) ν_4 region.

Many experiments were carried out to produce SiH_3 by microwave discharge of the silane in Ar or H_2 or D_2, by photolysis of a matrix with a hydrogen discharge through a LiF window, or irradiation with a deuterium lamp through a LiF window.

3. Results

CH_4 Observations. Because of differences in Coriolis coupling, ϵ, in the ν_3 (asym. str.) and ν_4 (bending) regions, the gas-phase rotational−vibrational bands of CH_4 show markedly different spacings.[33] Nominally they would be $2\tilde{B} = 10.5$ cm^{-1} apart; however, $\epsilon_3 = +0.05$ and $\epsilon_4 = +0.45$ so that only ν_3 approaches that spacing. The observed lines are P(1), Q(1), R(0), and R(1), with a spacing of 10.0 cm^{-1} for ν_3 and 5.7 cm^{-1} for ν_4. In an argon matrix, FE measured average spacings of 6.3 (2.0) for ν_3 and 3.8 (0.14) cm^{-1} for ν_4. JES obtained similar spectra for ν_4 in argon. Those authors considered Coriolis and crystal field effects and concluded that CH_4 is a hindered rotor in solid argon at 4 K.

CH_4/Ar. Our spray-on results at 4 K for CH_4 in solid argon 0.1 mol % (M/A = 1000), with 0.1% O_2 also present, are shown in Figures 1 and 2. Figure 2 is about 20 min after Figure 1, at 4 K. Without the O_2 catalyst, these nuclear spin changes would take several hours. These spectra are not too different from those of FE. The ν_4 spectra in Figure 1b is exactly the same as that in the higher resolution spectra of JES. The triplet R(0) transitions are explained by them as due to two sites, with the R(0) band among the rotational transitions being the most intense

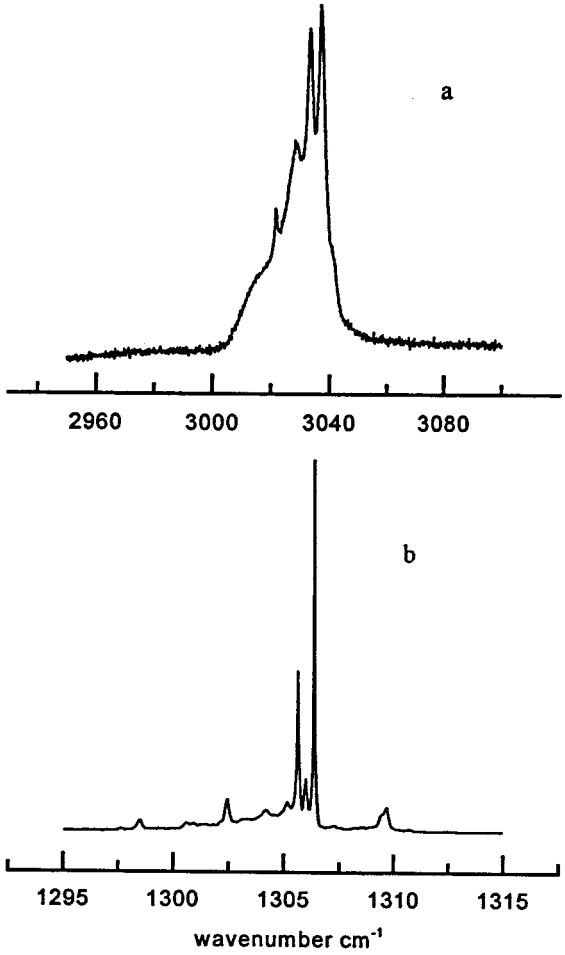

Figure 2. Same as Figure 1 but 20 min later.

at 1306.39 cm^{-1}. Figure 2 shows clearly the dominance of the R(0) bands as spin conversion occurs. The weaker ν_3 band is broad, as FE also note, and the R(1) line is only a shoulder, as is also the case in their study. There are some broad underlying features in these figures, which a more dilute matrix than 0.1 mol % might remove. However, our principal purpose here was to show that our deposition and spectroscopic procedures were satisfactory compared to the FE and MS procedure of condensation in a cell at 8 K.

CH_4/*n*-H_2. The spectra of 0.01% CH_4 in *n*-H_2 at 2 K are shown in Figure 3. A narrow (∼0.3 cm^{-1}) ν_4 band occurred at R(0) = 1308.2 cm^{-1} and a small reproducible Q(1) band at 1303.6 cm^{-1}. Clearly this is a spectrum where complete spin conversion has occurred, and a Boltzmann distribution prevails at 2 K. Presumably the presence of *o*-H_2 has catalyzed the conversion, but at this low concentration O_2 impurities might also be important. To support this, no change of the relative intensities with time was observed.

Correspondingly, the weaker ν_3 band in *n*-H_2 in Figure 3a is observed as essentially one band of overall width ∼2 cm^{-1}, centered at 3025 cm^{-1}. (MS from condensation of the liquid *p*-H_2 at 8 K observed the P(1), Q(1), R(0), R(1) bands at 3009, 3018, 3026, and 3031 cm^{-1}.)

Some differences were noted by Tam et al.[18] when CH_4/*p*-H_2 matrices were prepared by two-beam gas deposition at 2 K and by gas condensation in an enclosed cell at ∼8 K. Our procedure is different from either of these since, not only are we using *n*-H_2, but we use one-beam deposition of the premixed gases. So we made a few matrices prepared by mixing from two beams during condensation. In these cases our concentra-

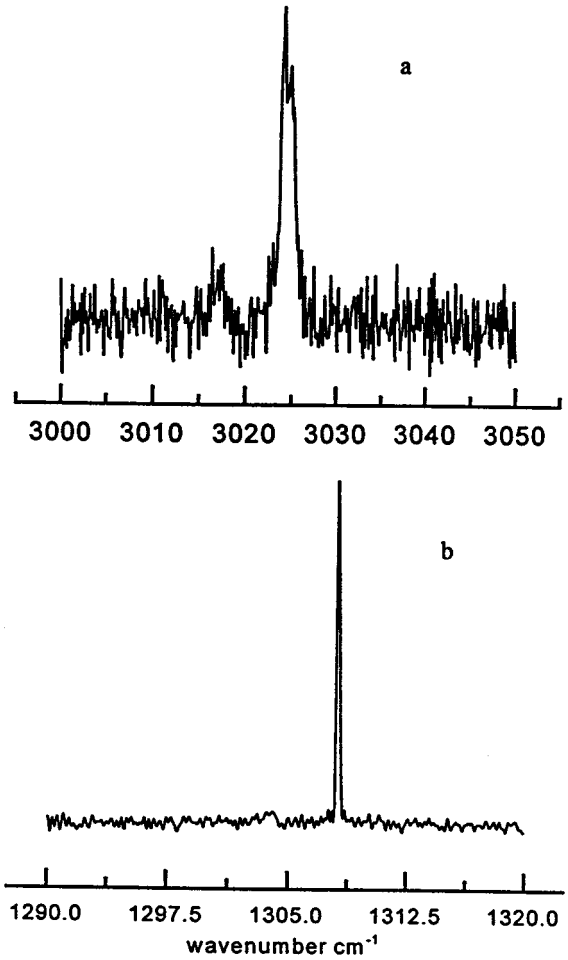

Figure 3. Absorption spectrum of 0.01 mol % (M/A = 10 000) CH_4 in solid *n*-H_2 at 2 K; (a) ν_3 region, (b) ν_4 region.

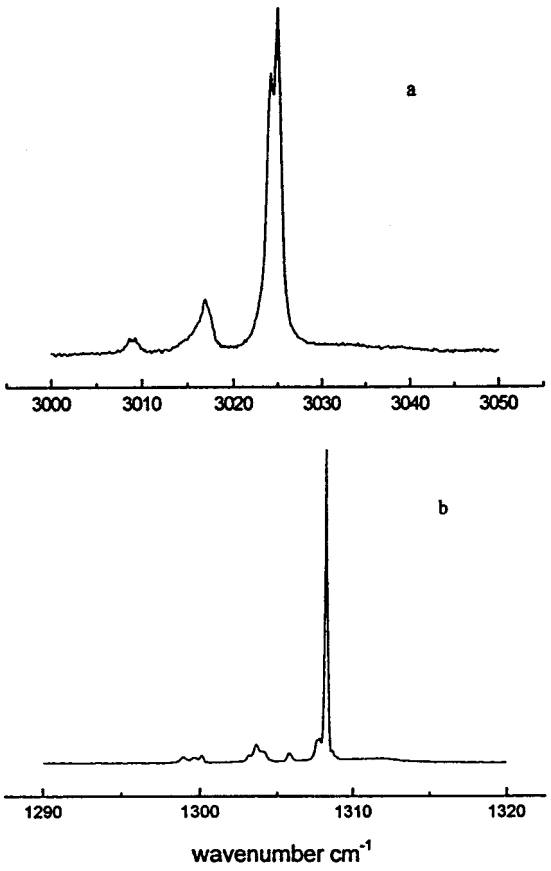

Figure 4. Absorption spectrum of CH_4 in solid *n*-H_2 (M/A ≅ 10 000) at 2 K, prepared by mixing gases just prior to condensation; (a) ν_3 region, (b) ν_4 region.

tions could only be estimated. We began with too concentrated an M/A, as indicated by the spectra, and lowered the flow of CH_4 relative to H_2 in successive runs. The most dilute spectrum (estimated as M/A ≅ 10 000) deposited and measured at 2 K is shown in Figure 4. These can be compared with the premixed spectra in Figure 3, which they approached over a period of 1/2 to 1 hour; i.e., all of the sidebands decrease relative to R(0) in Figure 3. However, these bands can be assigned to the P(1), Q (1), R(1) (broad) in the case of ν_4. The band at 1305.8 cm^{-1} is anomalous and could be the rotationless 0−0 transition, but it also decreases with time.

SiH_4/SiD_4 Observations. Similar to CH_4 in the gas phase, SiH_4, with $\tilde{B} = 2.86$ cm^{-1}, shows separations of the P(1), Q(1), R(0), R(1) lines of 5.6 cm^{-1} for ν_3 and 3.0 cm^{-1} for ν_4. (Here $\epsilon_3 = +0.022$ and ϵ_4 is estimated as $+0.478$).[32,33]

SiH_4/Ar. Judging by the gas-to-argon data from CH_4, one might expect the separations to be about 3 cm^{-1} for ν_3 and 1.5 cm^{-1} for ν_4 in an argon matrix. Also as noted above, if rotation and nuclear spin conversion have occurred (i.e., a Boltzmann distribution prevails), the transitions from $J = 1$ should be quite strong, about five times stronger than for CH_4 at 4 K.

Figure 5 shows the spectra of ν_3 and ν_4 of SiH_4 in argon at 4 K at a concentration of about 0.005 mol % (M/A = 20 000). Even at this high dilution, it is apparent that the spectrum includes background that is not due to isolated SiH_4 molecules. In the gas phase, $\nu_3 = 2189.1$ and $\nu_4 = 913.3$ cm^{-1}, which are the IR-active vibrations. Each of these frequencies would be expected to be lowered in an argon matrix so that it is logical to assign in the matrix the sharp bands $\nu_3 = 2176.8$ and $\nu_4 =$ one or both of the frequencies 905.1, 905.4 cm^{-1}.

At higher concentrations (0.05%, M/A = 2000), all of the sharper bands in Figure 5 persist, but now they are underlaid by very broad background extending over about 20 cm^{-1} for both ν_3 and ν_4 (Figure 6). Also appearing more clearly are the two small bands (doublets in the case of ν_4) just below 905.1 and 2176.8 cm^{-1} corresponding to the ^{29}Si, ^{30}Si isotopic species present in 4.7, 3.1% natural abundance. The positions of these isotopic bands are listed in Table 1. Figure 6 is essentially the same as Figure 5 of WSHS.

It is interesting that the broad and structured features in these two figures appear adjacent, and on the high-frequency side, to the strong sharp features that we would attribute to isolated SiH_4 in the argon matrix. It is difficult to assign these extra bands to impurities possibly resulting from silane reactions with background H_2O and CO_2.

The spectra of CH_4/Ar and SiH_4/Ar are quite different. The sharp features in the CH_4 spectra (Figure 1) can be accounted for by rotational structure, as discussed by FE and JES; whereas it appears that only the R(0) bands (or rotationless 0−0 transitions) of SiH_4 are observed. There appear to be no bands initiated from $J = 1$ in Figure 5a, which implies either that the nuclear-spin-conversion rate is very fast or that a catalyst is present in the gas mixture.

SiH_4/*p*-H_2, *n*-H_2. Figure 7 shows the ν_4 and ν_3 bands observed at 2 K for 0.01% (M/A = 10 000) SiH_4 in *p*-H_2. Deposition in *n*-H_2 gave the same spectrum. Deposition and measurement at 4 K led to enhancement of very weak features at 911.9, 910.6, 900.9, 900.0 cm^{-1}. Annealing these matrices was difficult and led to loss of the sample. The strongest peak

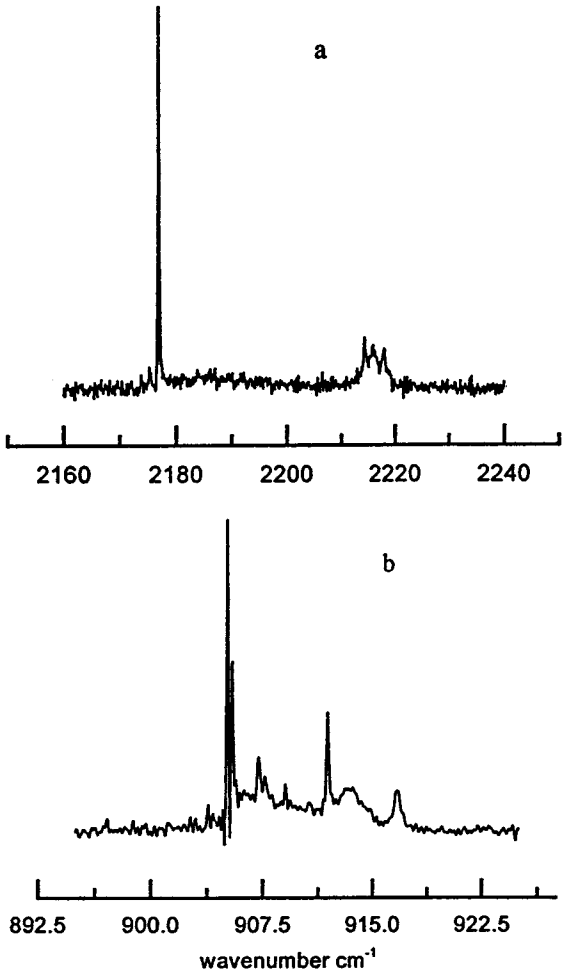

Figure 5. Absorption spectrum of 0.005 mol % (M/A = 20 000) SiH_4 in solid argon at 4 K; (a) ν_3 region, (b) ν_4 region.

in ν_4 occurs at 908.4 cm^{-1} and for ν_3 at 2190.6 cm^{-1}. The positions of the three bands (of decreasing intensity) near 908 cm^{-1} were 908.4, 908.9, and 909.8 cm^{-1} and are then assigned as sites, as is also the band at 2184 cm^{-1}.

SiH_4/D_2. Figure 8 a,b are ν_3 and ν_4, respectively, of 0.05% SiH_4 (M/A = 2000) in D_2 at 4 K. At first glance, the bands in Figure 8b appear to be rotational structures, but there is no structure on the broader (fwhh $\cong$ 2 cm^{-1}) ν_3 band. The five ν_4 bands are spaced at 905.5, 906.7, 907.5, 908.0, and 908.5 cm^{-1}. Evidence against rotational structure is also given by SiD_4/D_2 spectra (see below Figure 11), which, although the centers of ν_3 and ν_4 are shifted, looks essentially the same as Figure 8. There, the spacings, expected to be smaller for rotating SiD_4, are about the same as in Figure 8.

One can attribute the bands at 905.5 and 906.7 cm^{-1} to ^{30}Si, ^{29}Si isotopic effects. They are much less evident in the ν_3 spectrum. (These isotopic satellites are much clearer in Figure 11a for SiD_4/D_2.) Their intensity should be about 8% of the total.

Observation of these bands at 5 K for 4 1/2 hours showed no intensity changes, and the spectra are interpreted as a Boltzmann distribution of $J = 0$ and $J = 1$ levels at 4 K.

SiD_4/Ar. The spectra, as shown in Figure 9, are similar to those of SiH_4/Ar but with ν_4 = 668.5, 668.8 cm^{-1} and ν_3 = 1588.7 cm^{-1}; however, the concentration was higher 0.1% (M/A = 1000). Again, there is evidence of additional structure on the high-frequency side of the sharp lines attributed to isolated molecules. Note that the extra bands lie closer to the isolated

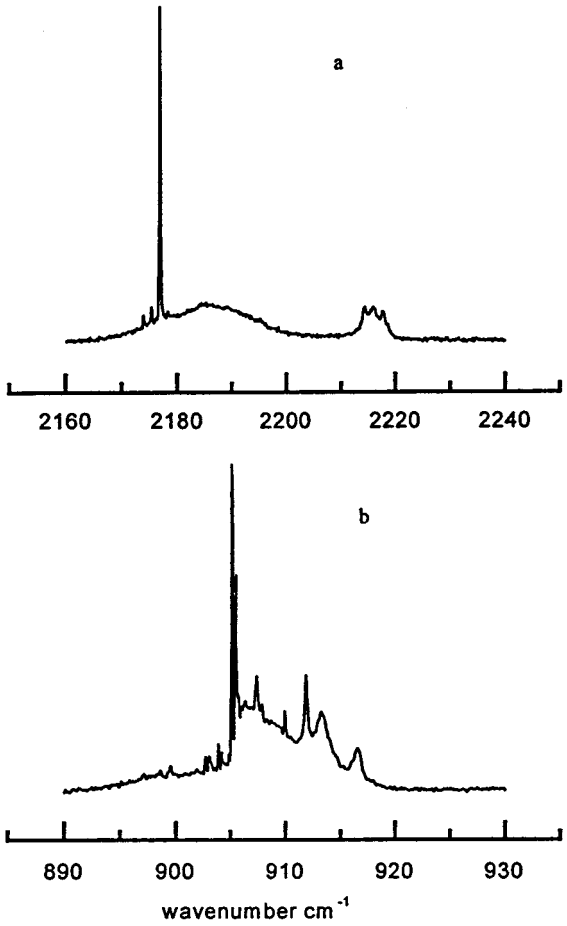

Figure 6. Same as Figure 5, but at a concentration of 0.05 mol % (M/A = 2000).

TABLE 1: Silicon Isotopic Shifts

				Teller−Redlich Ratios[a]			
				30/28		29/28	
	28	29	30	expt.	theory	expt.	theory
SiH_4/Ar							
ν_4	905.14	903.86	902.67				
ν_3	2176.84	2175.30	2173.91	0.99593	0.99580	0.99788	0.99783
SiH_4/D_2							
ν_4	908.0	906.7	905.5				
SiD_4/Ar							
ν_4	668.5	666.9	665.5				
ν_3	1588.7	1586.5	1584.4	0.99282	0.99252	0.99623	0.99614
SiD_4/D_2							
ν_4	670.8	669.3	667.8				
ν_3	1593.4	1591.2	1589.1	0.99284	0.99252	0.99639	0.99614

[a] $\nu_3^i\nu_4^i/\nu_3^{28}\nu_4^{28}$ [see page 235, equation (II, 328) in ref 40].

frequencies in this deuterated molecule than in SiH_4. Again ^{29}Si and ^{30}Si bands are observed at 1586.5 and 1584.4 cm^{-1} and at 666.9 and 665.5 cm^{-1} (see Table 1).

SiD_4/*n*-H_2. Two strong single bands, of width about 2 cm^{-1}, at 671.8 and 1598.1 cm^{-1} are shown in Figure 10. The concentration of SiD_4 was 0.013% (M/A = 7700) and the deposition temperature was ~2 K. This matrix was successfully annealed to 4−6 K. In Figure 10b, the shoulder at ~674 cm^{-1} and the weak band 665 cm^{-1} grow, as do also the weak features at 1603, 1594, 1592.4, 1588.4 cm^{-1} in Figure 10a.

SiD_4/D_2. Figure 11 shows the spectra of 0.11 mol % (M/A = 900) of SiD_4 in solid deuterium at 4 K. As mentioned earlier, it is similar to Figure 8 of SiH_4/D_2. Here, ν_3 = the doublets at 670.5, 670.8 cm^{-1} and ν_4 = 1593.4 cm^{-1} (a shoulder also

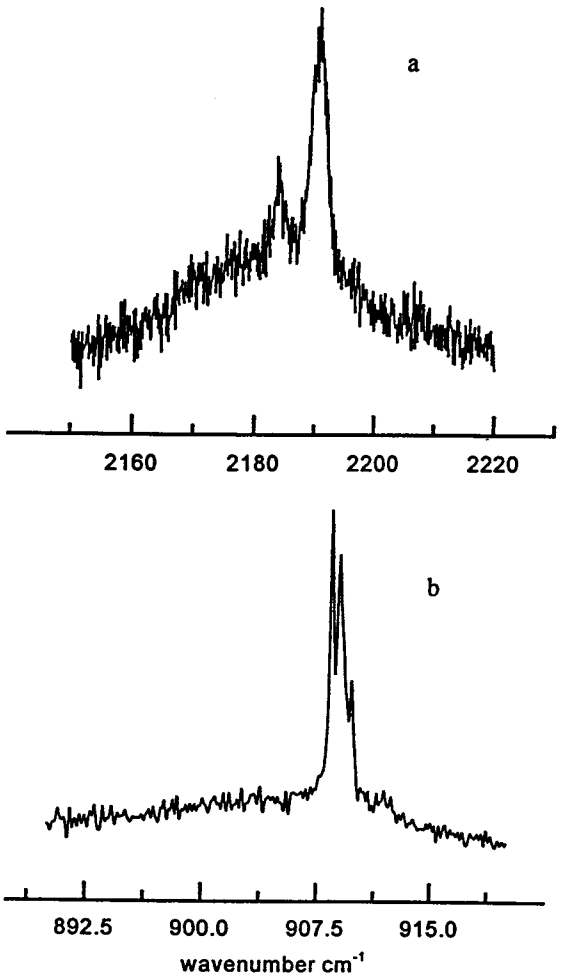

Figure 7. Absorption spectrum of 0.01 mol % (M/A = 10 000) SiH_4 in solid *p*-H_2 at 2 K; (a) ν_3 region, (b) ν_4 region.

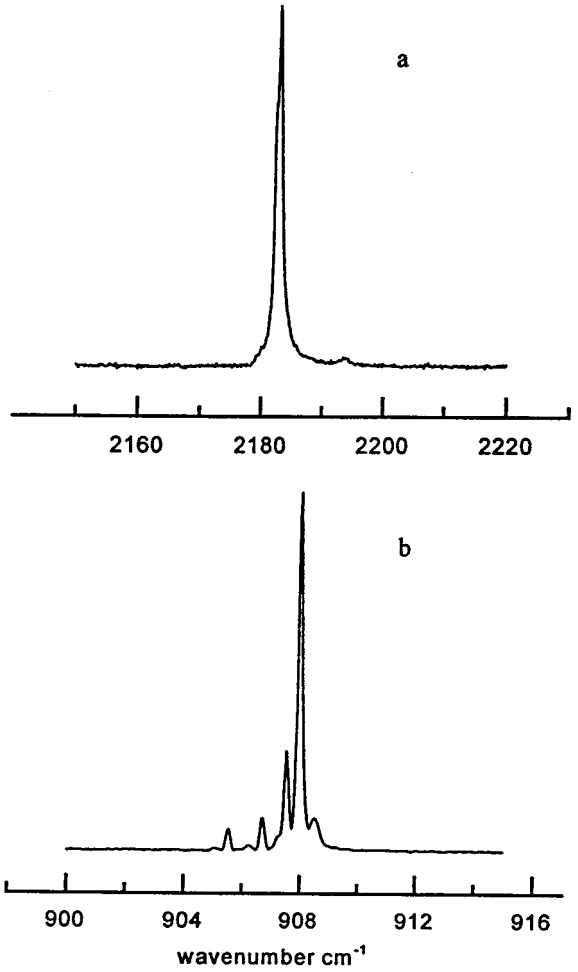

Figure 8. Absorption spectrum of 0.05 mol % (M/A = 2000) SiH_4 in solid D_2 at 4 K; (a) ν_3 region, (b) ν_4 region.

indicates that it is a doublet). The two sharp lines at 669.3, 667.8 cm^{-1} and 1591.2, 1589.1 cm^{-1} can be assigned to the ^{29}Si, ^{30}Si molecules (see Table 1). One interprets this as the spectrum of an isolated SiD_4 molecule. There was no variation of the spectrum with time.

SiH_3 Radical. Plasmas containing silane have been customarily used to prepare silicon devices, and therefore there have been extensive investigations of the radicals produced and their reactions. The literature is too numerous to reference here, but both experimental and theoretical studies of individual silyl radicals have been made.

SiH_3 is a pyramidal molecule with four IR-active vibrations, only two of which have been observed at 725 cm^{-1} (ν_2, average of doublet)[35] and 2185 cm^{-1} (ν_3) in the gas phase. Theoretically calculated frequencies were done by Bunker and Olbrich[41] and Allen and Schaefer.[37] The latter give $\nu_1 = 2150$, $\nu_2 = 773$, $\nu_3 = 2180$, $\nu_4 = 933$ cm^{-1}. The IR of SiH_3 has not been identified in rare-gas matrices, but weak bands at ~730 and 930 cm^{-1} in the spectra obtained by Lloret and Abouaf-Marguin[24,29] from a hot cathode discharge of SiH_4/Ar are probably it. Si_2H_6 bands at 836 and 940 cm^{-1} were also observed there.[42] The 2100 cm^{-1} bands are difficult to identify since they lie among the usually dominant SiH_4 bands. The ESR of SiH_3 has been observed by many workers, beginning with the studies by Gordy and coworkers in 1966.[43,44]

We were encouraged by the strong ESR signals of SiH_3 in solid Ar produced by Raghunathan and Shimokoshi[45] using a hydrogen discharge lamp as a radiation source to dissociate SiH_4. [The silyl halides were not available (SiH_3I must be synthesized), and furthermore we wished to avoid the perturbations by I or Cl atoms in the matrix.]

Many runs were made with SiH_4 or SiD_4 in argon, hydrogen, and deuterium matrices with irradiation during or after deposition with a hydrogen microwave discharge or deuterium lamp through a LiF window. Figure 12 shows the band at 545.8 cm^{-1} for SiD_3 in solid D_2 at 4 K and the much stronger bands at 619.5 and 679.2 cm^{-1} due to the dimer Si_2D_6. SiD_3 and SiH_3 were also observed in Ar at 545.5 and 733.6 cm^{-1}, respectively. The dimer bands were always very strong, more-or-less independent of the original silane concentration in the matrix.

4. Discussion

Let us consider the argon spectra first.

SiH_4, SiD_4/Ar. As noted, the spectra of the silane molecules (Figures 5, 6, and 9 at 4 K) do not contain transitions from the $J = 1$ levels as observed in the CH_4 spectra (Figures 1 and 2 at 4 K). This is particularly evident for the ν_3 band in Figures 5a, 6a, and 9a where, except for weak isotopic doublets, nothing appears on the low-frequency side of the intense sharp bands. If rotating, whether in a non-equilibrium nuclear spin state or if a Boltzmann distribution at 4 K prevails, transitions from $J = 1$ states should be readily observed. (See the earlier discussion under nuclear spin conversion.) The bandwidth of ν_3 in Figures 5, 6, and 9 is about 0.3 cm^{-1} so that the absence of P(1), Q(1) branches is definite. One must then attribute the strong sharp bands in these spectra as (0−0) transitions of rotationless

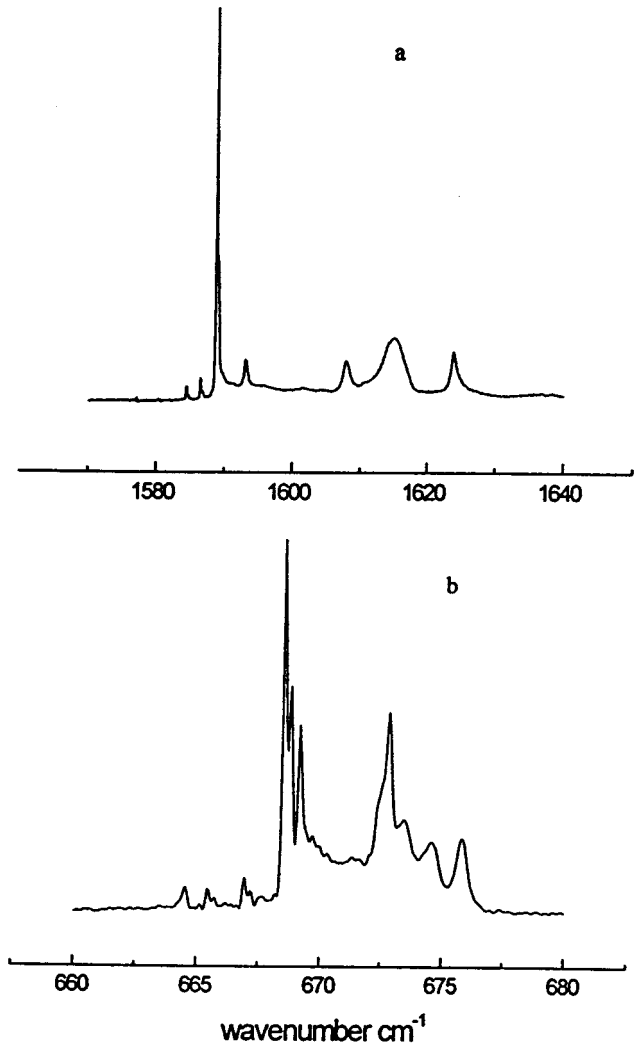

Figure 9. Absorption spectrum of 0.1 mol % (M/A = 1000) SiD_4 in solid argon at 4 K; (a) ν_3 region, (b) ν_4 region.

molecules or ones which are highly rotationally hindered, as observed by Redington and Milligan[38] for H_2O.

SiH_4 has a bond distance of 1.48 Å as compared to 1.092 Å in CH_4. These may be roughly interpreted as van der Waals diameters of 3.7 and 2.7 Å, respectively, to be compared with a substitutional site in solid argon of 3.76 Å[46] and in hcp solid hydrogen of ~3.78 Å. Thus, SiH_4 is a tighter fit than CH_4. It is spherical but its polarizability is higher than CH_4 so that the attractive interaction with the surrounding matrix is higher, thus apparently preventing its rotation.

Also interesting is the appearance of structure on the high frequency side of the (0−0) bands, more so for the bending ν_4 than the stretching ν_3. This suggests that this structure is due to coupling of molecular vibrations with matrix (argon) lattice vibrations (phonons). The sideband structure is more evident in Figure 6 where the concentration of SiH_4 in argon is increased to 0.05 mol % (M/A = 2000). As discussed elsewhere,[47] phonon sidebands may appear as broad multiphonon or discrete bands on the high frequency side of the zero-phonon bands in the absorption spectra. Here the zero-phonon bands of SiH_4 are identified as the (0−0) bands at 2176.8 and 905.1 cm^{-1} in Figures 5 and 6, and for SiD_4 at 1588.7 and 668.5 cm^{-1} in Figure 9. It is noteworthy that this coupling is stronger with the lower ν_4 bending than with the stretching ν_3, as one might expect. Annealing did sharpen some features of the sideband structures

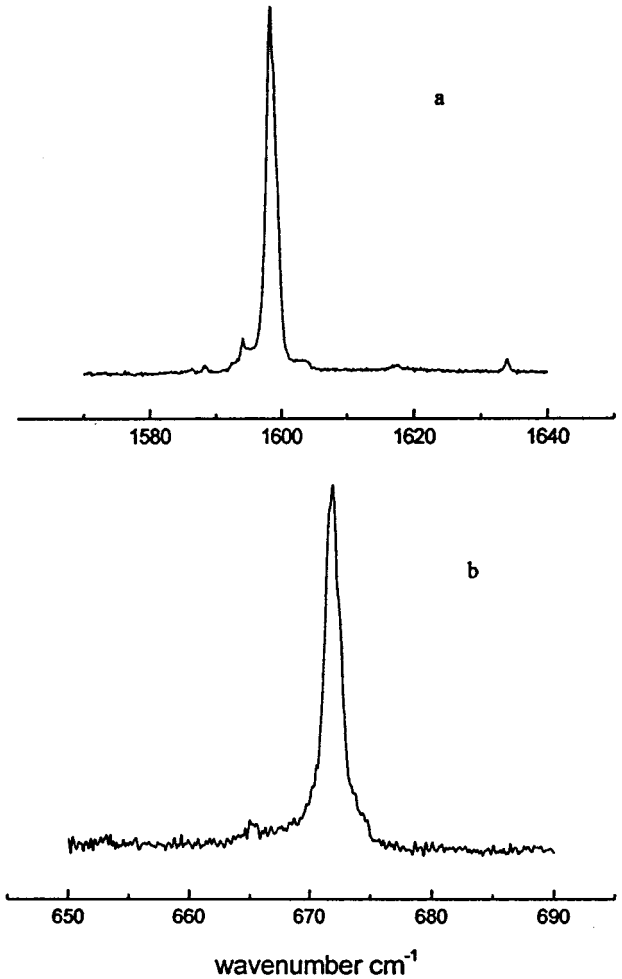

Figure 10. Absorption spectrum of 0.013 mol % (M/A = 7700) SiD_4 in solid *n*-H_2 at 2 K; (a) ν_3 region, (b) ν_4 region.

in the ν_4 region of both silanes. The phonon structure is complex, implying different sites of interaction in these polycrystalline matrices.

SiH_4, SiD_4/H_2, D_2. To maintain a stable matrix, all H_2 experiments were performed at 2 K, but this was not necessary for D_2. The rotational Boltzmann factors ($J = 1/J = 0$) are affected greatly by this temperature change: at 2 K, 0.05 for SiH_4, 0.4 for SiD_4; at 4 K, 0.4 for SiH_4, 1.0 for SiD_4 (SiD_4 having twice the moment of inertia of SiH_4). Thus, if SiH_4 is rotating at 2 K, any bands due to transitions from $J = 1$ levels should be very weak, if observable, relative to the R(0) band. However, for SiH_4 at 4 K and SiD_4 at either temperature, the $J = 1$ levels are highly populated and even more highly populated if nuclear spin conversion is slow.

Since $J = 1$ transitions are not discernible in Figures 7 and 8, the general statement can be made that nuclear spin relaxation in SiH_4 has occurred, i.e., that the conversion is rapid. Furthermore, their absence at 4 K (Figure 8) implies that SiH_4 is not rotating, so the large bands in both figures are (0−0) rotationless transitions. Again, no $J = 1$ trasitions are observed for SiD_4 in Figures 10 and 11, where they should be prominent if the molecule is rotating.

The general conclusions are (1) nuclear-spin relaxation in SiH_4 is rapid and (2) the silane molecules are not rotating at 2 or 4 K in argon, H_2, D_2 matrices.

A list of all of the main (0−0) bands in Ar, H_2, and D_2 matrices is given in Table 2 along with the calculated values of the Teller−Redlich ratio for $^{28}SiH_4/^{28}SiD_4$. As expected, because

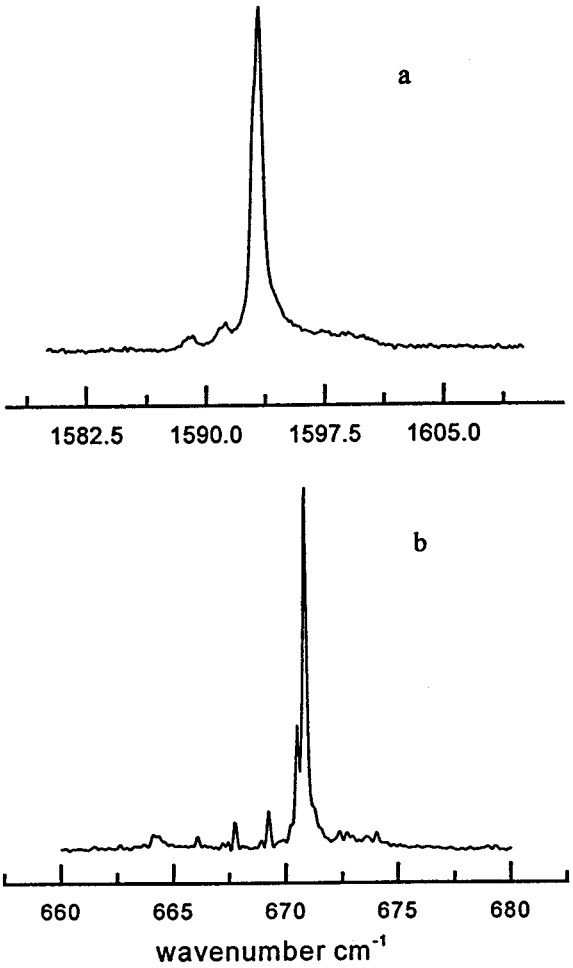

Figure 11. Absorption spectrum of 0.11 mol % (M/A = 900) SiD_4 in solid D_2 at 4 K; (a) ν_3 region, (b) ν_4 region.

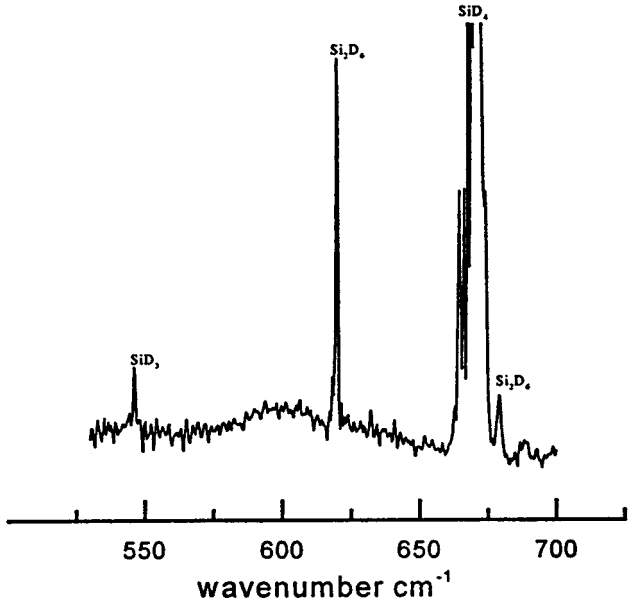

Figure 12. Absorption spectrum of a matrix of 0.1 mol % (M/A = 1000) SiD_4 in solid D_2 irradiated with H_2 discharge emission during deposition at 4 K.

of anharmonicity, those ratios are all greater than the theoretical harmonic value, 0.5309. A similar application of T−R theory to the ^{29}Si, ^{30}Si satellites is given in Table 1.

SiH_3/SiD_3. The formation of these radicals by irradiation with a hydrogen microwave emission always led to the formation of the dimer Si_2H_6/Si_2D_6 and was logically attributed to diffusion of SiH_3 radicals. However, this occurred in both the relatively rigid Ar and the softer hydrogen matrices, and it may be that the detected disilane could be formed predominately from two adjacent SiH_4 molecules in a concerted reaction:

$$2SiH_4 \xrightarrow{h\nu} Si_2H_6 + H_2$$

and that hydrogen discharge radiation is not efficient in producing SiH_3 from monomeric silane.

TABLE 2: ν_3 and ν_4 Bands of Isolated $^{28}SiH_4$ and $^{28}SiD_4$ in Various Matrices

	$^{28}SiH_4$		$^{28}SiD_4$		
matrix	ν_3	ν_4	ν_3	ν_4	T−R ratio[a]
gas	2189.1	913.3	1589	681	0.5412
argon	2176.8	905.1	1588.7	668.5	0.5390
H_2	2189.8	908.4	1598.1	671.8	0.5397
D_2	2182.9	908.0	1593.4	670.8	0.5393

[a] Teller−Redlich ratio $\nu_3^D\nu_4^D/\nu_3^H\nu_4^H$ [see page 235, equation (II, 328), in ref 40]. Theory predicts a ratio of 0.5309 for harmonic frequencies.

Acknowledgment. This research was supported by the National Science Foundation (Grant CHE-9726297). Acknowledgment is also made to the donors of the Petroleum Research Fund, administered by the American Chemical Society, for support of this research (ACS−PRF Grant 34820-AC.).

References and Notes

(1) Frayer, F. H.; Ewing, G. E. *J. Chem. Phys.* **1967**, *46*, 1994. Frayer, F. H.; Ewing, G. E. *J. Chem. Phys.* **1968**, *48*, 781.
(2) Curl, R. F., Jr.; Kasper, J. V. V.; Pitzer, K. S. *J. Chem. Phys.* **1967**, *46*, 3220.
(3) Hopkins, H. P., Jr.; Donoho, P. L.; Pitzer, K. S. *J. Chem. Phys.* **1967**, *47*, 864.
(4) Hopkins, H. P., Jr.; Curl, R. F., Jr.; Pitzer, K. S. *J. Chem. Phys.* **1968**, *48*, 2959.
(5) Vogt, G. J.; Pitzer, K. S. *J. Chem. Thermodyn.* **1976**, *8*, 1011.
(6) Nanba, T.; Sagara, M.; Ikezawa, M. *J. Phys. Soc. Jpn.* **1980**, *48*, 228.
(7) Buchman, S.; Candela, D.; Vetterling, W. T.; Pound, R. V. *Phys. Rev. B* **1982**, *26*, 1459.
(8) Nelander, B. *J. Chem. Phys.* **1985**, *82*, 5340.
(9) Baciocco, G.; Calvani, P.; Cunsolo, S. *Chem. Phys. Lett.* **1986**, *132*, 410.
(10) Jones, L. H.; Eckberg, S. A.; Swanson, B. I. *J. Chem. Phys.* **1986**, *85*, 3203.
(11) Jones, L. H.; Eckberg, S. A. *J. Chem. Phys.* **1987**, *87*, 4368.
(12) Hepp, M.; Winnewisser, G.; Yamada, K. M. T. *J. Mol. Spectrosc.* **1994**, *164*, 311.
(13) Momose, T.; Uchida, M.; Sogoshi, N.; Miki, M.; Masuda, S.; Shida, T. *Chem. Phys. Lett.* **1995**, *246*, 583.
(14) Momose, T.; Miki, M.; Wakabayashi, T.; Shida, T.; Chan, M.-C.; Lee, S. S.; Oka, T. *J. Chem. Phys.* **1997**, *107*, 7707.
(15) Momose, T.; Katsuki, H.; Hoshina, H.; Sogoshi, N.; Wahabayashi, T.; Shida, T. *J. Chem. Phys.* **1997**, *107*, 7717.
(16) Momose, T. *J. Chem. Phys.* **1997**, *107*, 7695.
(17) Momose, T.; Shida, T. *Bull. Chem. Soc. Jpn.* **1998**, *71*, 1.
(18) Tam, S.; Fajardo, M. E.; Katsuki, H.; Hoshina, H.; Wakabayashi, T.; Momose, T. *J. Chem. Phys.* **1999**, *111*, 4191.
(19) Galtsov, N. N.; Prokhvatilov, A. I.; Strzhemechny, M. A. *Low Temp. Phys.* **2000**, *26*, 676.
(20) Miki, M.; Momose, T. *Low Temp. Phys.* **2000**, *26*, 661.
(21) Govender, M. G.; Ford, T. A. *J. Mol. Struct.* **2000**, *550−551*, 445.
(22) Wilde, R. E.; Srinivasan, T. K. K.; Harral, R. W.; Sankar, S. G. *J. Chem. Phys.* **1971**, *55*, 5681.
(23) Kafafi Ismail, Z.; Hauge, R. H.; Fredin, L.; Kauffman, J. W.; Margrave, J. L. *J. Chem. Phys.* **1982**, *77*, 1612.
(24) Abouaf-Marguin, L.; Lloret, A. *J. Non-Cryst. Solids* **1985**, *77−78*, 761.
(25) Withnall, R.; Andrews, L. *J. Phys. Chem.* **1985**, *89*, 3261.
(26) Fredin, L.; Hauge, R. H.; Kafafi, Z. H.; Margrave, J. L. *J. Chem. Phys.* **1985**, *82*, 3542.

(27) Nakamura, K.; Masaki, N.; Sato, S.; Shimokoshi, K. *J. Chem. Phys*. **1985**, *83*, 4504.
(28) Van Zee, R. J.; Ferrante, R. F.; Weltner, W., Jr. *J. Chem. Phys*. **1985**, *83*, 6181.
(29) Lloret, A.; Abouaf-Marguin, L. *Chem. Phys*. **1986**, *107*, 139.
(30) Nakamura, K.; Okamoto, M.; Takayanagi, T.; Kawachi, T.; Shimokoshi, K.; Sato, S. *J. Chem. Phys*. **1989**, *90*, 2992.
(31) McKean, D. C.; Chalmers, A. A. *Spectrochim. Acta* **1967**, *23A*, 777.
(32) Kattenberg, H. W.; Oskam, A. *J. Mol. Spectrosc.* **1974**, *49*, 52.
(33) Johns, J. W. C.; Kreimer, W. A.; Susskind, J. *J. Mol. Spectrosc*. **1976**, *60*, 400.
(34) Makowe, J.; Boyarkin, O. V.; Rizzo, T. R. *J. Phys. Chem. A.* **2000**, *104*, 11505.
(35) Yamada, C.; Hirota, E. *Phys. Rev. Lett.* **1986**, *56*, 923.
(36) Gray, D. L.; Robiette, A. G.; Johns, J. W. C. *Mol. Phys.* **1977**, *34*, 1437.
(37) Allen, W. D.; Schaefer, H. F., III *Chem. Phys.* **1986**, *108*, 243.
(38) Redington, R. L.; Milligan, D. E. *J. Chem. Phys.* **1962**, *37*, 2162. Redington, R. L.; Milligan, D. E. *J. Chem. Phys.* **1963**, *39*, 1276.
(39) Steinhoff, R. A.; Apparao, K. V. S. R.; Ferguson, D. W.; Rao, K. N.; Winnewisser, B. P.; Winnewisser, *M. Can. J. Phys.* **1994**, *72*, 1122.
(40) Herzberg, G. *Infrared and Roman Spectra of Polyatomic Molecules*; Van Nostrand: New York, 1945.
(41) Bunker, P. R.; Olbrich, *G. Chem. Phys. Lett.* **1984**, *109*, 41.
(42) Bethke, G. W.; Wilson, M. K. *J. Chem. Phys.* **1957**, *26*, 1107.
(43) Morehouse, R. L.; Christiansen, J. J.; Gordy, W. *J. Chem. Phys.* **1966**, *45*, 1751.
(44) See Van Zee, R. J.; Ferrante, R. F.; Weltner, W., Jr. *J. Chem. Phys.* **1985**, *83*, 6181 for later references.
(45) Raghunathan P.; Shimokoshi, *K. Spectrochim. Acta A* **1980**, *36*, 285.
(46) Pollack, G. L *Rev. Mod. Phys.* **1964**, *36*, 748.
(47) Li, S.; Weimer, H. A.; Van Zee, R. J.; Weltner, W., Jr. *J. Chem. Phys.* **1997**, *106*, 2583.